Robotica (2005) volume 23, pp. 75–81. © 2005 Cambridge University Press
DOI: 10.1017/S0263574704000670 Printed in the United Kingdom

Design and simulation of a class of spatial reactionless manipulators

Abbas Fattah* and Sunil K. Agrawal

Mechanical Systems Laboratory, Department of Mechanical Engineering, University of Delaware, Newark, DE 19716 (USA)
E-mail: fattah, agrawal@me.udel.edu

(Received in Final Form: May 30, 2004)

SUMMARY
For conventional designs of robots, manipulator motions result in forces and moments on the base. These forces and moments may cause undesirable translation and rotation of the base. The objective of this paper is to systematically analyze the fundamentals of reactionless robots. Based on this analysis, a design of one distinct class of spatial robot is proposed. The design is achieved through appropriate choices of geometric and inertial parameters. Due to the underlying conservation laws, the trajectory must satisfy additional constraints. We illustrate the reactionless feature of this robot through computer simulations. We are also fabricating reactionless robots to illustrate the underlying concepts.

KEYWORDS: Reactionless manipulators; Spatial robots; Constraints.

1. INTRODUCTION

In the literature, a number of methods have been proposed for static balancing of machines through passive means using counterweights and springs. These methods have been applied to linkages,[1–3] serial and direct-drive manipulators[4–7] and parallel mechanisms.[8,9] The center of mass is an important property of a machine. Force balancing of machines is achieved by ensuring that the system center of mass remains stationary during motion.[1] In recent years, Gokce and Agrawal[10] revised this concept. Subsequently, they fabricated a design where the center of mass of the system was located appropriately through the addition of parallelogram linkages.[11]

Research has been reported on dynamic balancing of linkages, especially with four-bars.[12–16] Counterweights or idler-loops are used to minimize forces and moments transmitted to the base. Also, dynamically balanced parallel mechanisms have been designed which use reactionless four-bar linkages in their legs[17,18] or have counter rotations with proper choice of geometric and inertia parameters.[19,20] Moreover, there are some published works on the open loop systems using trajectory planning to obtain reactionless manipulators or minimize moments transmitted to the base.[21,22] The issue of reactionless control of a space robot keeping the base inertially fixed was proposed in references [23,24]. Another research work was presented in reference [25] to design the Hummingbird minipositioner to be dynamically balanced. In this work, the authors fixed the location of the center of mass of the machine to make the system statically balanced using the appropriate relations among the inertia parameters. Then using the fact that the links and all other accessories are symmetric about some reference plane, they concluded that there is only one nonzero moment about the axis perpindicular to the plane. They cancelled this moment by introducing counteracting torques through the use of a toque adjustable motor. However, their method took advantage of the symmetry in order to vanish the moments transfered to the base. This is not applicable to a general mechanism. Also, extra actuators reduce the system's manipulation capabilities.

In most research, dynamic balancing of the mechanisms is attained by proper choice of geometric and inertial parameters, appropriate trajectory planning and adding counter rotations or counteracting torques with a proper controller. A significant difference in this paper is that this property is achieved through the use of a new class of spatial manipulators using auxiliary parallelograms as well as passive joint connection between manipulator and the base.

The main contributions of this paper are:

(i) *design and simulation study of a class of spatial manipulators using auxiliary parallelograms. This design is simpler in terms of links, complexity of the added masses, and inertia to the system, than conventional designs using counterweights;*
(ii) *attainment of zero moment transmission to the base along specified axes through an appropriate choice of passive joints.*

The organization of the paper is as follows: Section 2 reviews the dynamic behavior of coupled bodies in open-chain configuration and uses these dynamic equations to find the necessary and sufficient conditions for the design of reactionless machines. Based on the underlying mathematics, a spatial open chain robot using auxiliary parallelograms is outlined in Section 3. Detailed mathematical models and simulation are presented for this design in Section 4.

* Corresponding author

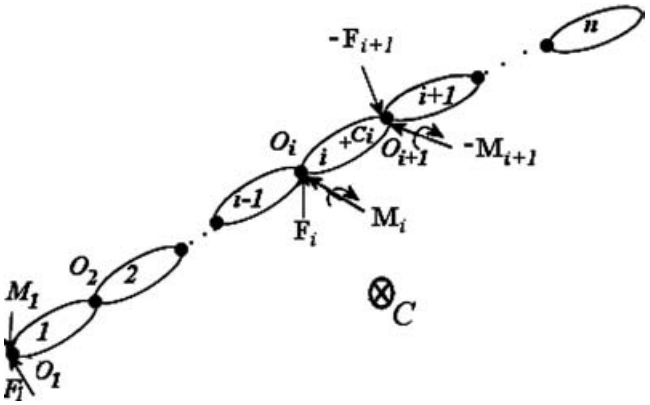

Fig. 1. An open chain of bodies.

2. THEORETICAL BACKGROUND AND REACTIONLESS MANIPULATORS

We study robots in an open chain. The bodies are numbered from 1 through n as shown in Fig. 1. We consider the body i in the chain to be connected to body $i-1$ at O_i and to $i+1$ at O_{i+1}. The center of mass of the body i is labeled as C_i. At the interconnection point O_i, the force and moment applied on body i from $i-1$ are respectively labeled as $\mathbf{F}_i$ and $\mathbf{M}_i$.

The motion of the overall system is characterized by the following two equations:

$$\mathbf{F}_1 + Mg\mathbf{n} = M\mathbf{a}_C, \tag{1}$$

$$\frac{d}{dt}\mathbf{H}_C = \mathbf{M}_1 + \mathbf{r}_{CO_1} \times \mathbf{F}_1, \tag{2}$$

where $\mathbf{H}_C$ is the net angular momentum vector around the system center of mass C, M is the total mass of the system defined as $\sum_{i=1}^{n} m_i$ and $\mathbf{r}_{CO_1}$ is a vector from C to O_1. The expression for $\mathbf{H}_C$ is

$$\mathbf{H}_C = \sum_{i=1}^{n} \left[\mathbf{I}_{C_i} \cdot \omega_i + \mathbf{r}_{CC_i} \times m_i \mathbf{v}_{C_i}\right], \tag{3}$$

where $\mathbf{v}_{C_i}$ is the velocity of the center of mass of C_i.

We assume that the contact between the system and the ground happens either at C or O_1. These two points may be the same in some cases. One can now make the following observations for a single contact system:

If $\mathbf{a}_C = 0, \mathbf{v}_{CM}$ is a constant. Since a machine at some initial time is at rest, this constant must be zero. This condition also implies that the center of mass of the machine is inertially fixed.

Through counterbalancing, it is possible to design a machine such that its center of mass is at O_1 where it is connected to the ground. Counter balancing of the chain must start out from the last body. The center of mass of body n must be placed on the joint axis connecting n and $n-1$. On carrying out this procedure successively to other bodies in the chain, the center of mass of the whole system will get placed on the joint axis between bodies 0 and 1. As a result, the center of mass becomes inertially fixed during entire motion.[9,15]

The second design for making the system center of mass C inertially fixed is determined as follows: First, the system center of mass is determined using auxiliary parallelograms [11]. Next the machine is connected to the base at the center of mass of the system such that it becomes an inertially fixed point. Section 3 outlines an example of this class of spatial manipulators which uses auxiliary parallelograms to locate the center of mass. In both designs, $\mathbf{F}_1 = -Mg\mathbf{n}$ from Eq. (1) and the force transmitted to the ground is a non-zero constant equal to $Mg\mathbf{n}$.

In this paper, the second design will be used because it is simpler, in terms of number of links, complexity of added masses and inertia to the system, when compared to the first design using counterbalancing.

If the center of mass of the machine is inertially fixed, then from Eq. (2),

$$\mathbf{M}_1 = \frac{d}{dt}\mathbf{H}_C \tag{4}$$

Now, two distinct cases are possible:

(I) Through proper choice of geometric and inertial parameters, the machine is designed so that $\mathbf{H}_C = 0$.[1,17] In this case, $\mathbf{M}_1 = 0$;

(II) If the connection between body 1 and O is through passive single or multiple degree-of-freedom joints, appropriate transmitted components of the moment between the system and the ground are zero. For example, if the connection at the center of mass between the system and the ground is through ball and socket joint, $\mathbf{M}_1 = 0$, i.e. there is no moment transfer between them. In this case, $\frac{d}{dt}\mathbf{H}_C = 0$. This will result in three scalar constraints to be satisfied by motion of the system. *In this case, the ground reaction is a constant and the ground moment is zero.*

Similarly, if the connection at C was through a revolute joint, then $\frac{d}{dt}\mathbf{H}_C \cdot \mathbf{b} = 0$, where $\mathbf{b}$ is a unit vector along the axis of the revolute joint. *The ground reaction is a constant and one component of the ground moment* $\mathbf{H}_C \cdot \mathbf{b} = 0$. The motion of the system is characterized by one scalar angular momentum conservation equation.

In this paper, the emphasis is to attain zero moment transmission along some specified axes through an appropriate choice of passive joints.

In the presence of external forces and moments on the system, in order to have a reactionless system, we should add appropriate thrusters to the system to keep the center of mass of system fixed. The thrusters should be designed such that it can be adjusted with the amount of external forces and moments exerted on the system.

3. MANIPULATOR WITH AUXILARY PARALLELOGRAMS

In this section, we illustrate the design with a class of spatial manipulators with auxiliary parallelograms that locate the center of mass, as shown in Fig. 2.[11] The center of mass is then used as the connection point for the system to the inertial frame by a revolute joint. The center of mass of the

https://doi.org/10.1017/S0263574704000670 Published online by Cambridge University Press

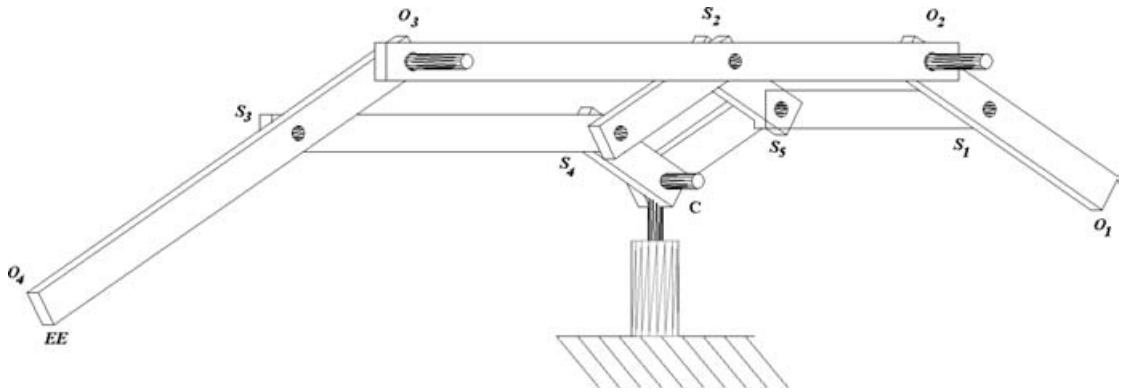

Fig. 2. A spatial manipulator with auxiliary parallelograms.

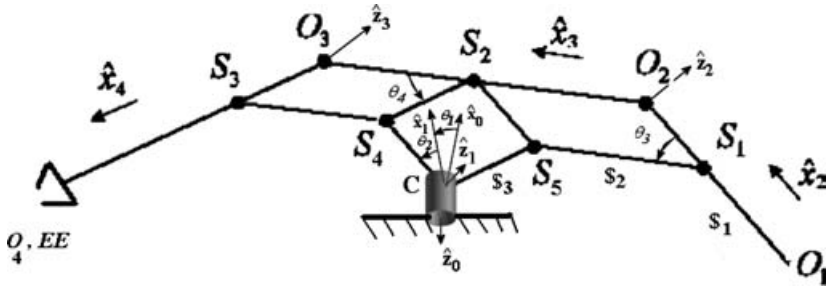

Fig. 3. Modeling of spatial manipulator with auxiliary parallelograms.

manipulator is located using a set of auxiliary parallelograms, as shown in Fig. 3. A set of scaled lengths $\$_i$ are computed from the description of the mechanism to construct the parallelograms and locate the center of mass of the whole system. Hence, the center of mass C becomes the inertially fixed point.

In this design, we consider three links with three auxiliary parallelograms which are connected to joint 1 at C as shown in Fig. 2. Joints 1 and 2 are located at C. The axes of joints 2, 3 and 4 are parallel to each other and are along $\hat{\mathbf{z}}_1$. The axis of joint 1 is along $\hat{\mathbf{z}}_0$ and is perpendicular to the axes of all three joints. An inertial frame $\mathcal{F}_0$ is located at C consisting of unit vectors $\hat{\mathbf{x}}_0, \hat{\mathbf{y}}_0, \hat{\mathbf{z}}_0$. A coordinate frame $\mathcal{F}_i$ is at point O_i with unit vectors $\hat{\mathbf{x}}_i$, $\hat{\mathbf{y}}_i$ and $\hat{\mathbf{z}}_i$. Link i is denoted by $O_i O_{i+1}$ for $i = 1, 2, 3$. Auxiliary links are defined as: $\overline{l}_{1a} = 1\overline{a} = S_5S_2 = CS_4$, $l_{2a} = 2a = S_1S_5$, $\overline{l}_{2a} = 2\overline{a} = S_4S_3$ and $l_{3a} = 3a = S_5C = S_2S_4$. The joint 2 at C is passive and all other joints are actuated. Therefore, the moment transmitted to the ground along axis z_1 vanishes, i.e. $M^C_{z1} = 0$. The angular momentum of the whole system is derived about C in order to obtain the moment transmitted to the ground.

3.1. Angular momentum of manipulator

The inertial angular momentum of the system about point C expressed in frame $\mathcal{F}_1$ can be written as

$$
\begin{aligned}
H_C = {} & \dot{\theta}_1 \left[\sum_{i=1}^{9} \mathbf{I}_i \mathbf{z}_0 + \sum_{i=1}^{9} \overline{CC_i} \times (\hat{\mathbf{z}}_0 \times m_i \overline{CC_i}) \right] \\
& + \dot{\theta}_2 \left[\sum_{i=1}^{9} \mathbf{I}_i \hat{\mathbf{z}}_1 + \sum_{i=1}^{9} \overline{CC_i} \times (\hat{\mathbf{z}}_1 \times m_i \overline{O_1 C_i}) \right] \\
& + \dot{\theta}_3 \left[\sum_{i=2, i\neq 4,5}^{9} \mathbf{I}_i \hat{\mathbf{z}}_2 + \sum_{i=2, i\neq 4,5}^{9} \overline{CC_i} \times (\hat{\mathbf{z}}_2 \times m_i \overline{O_2 C_i}) \right] \\
& + \dot{\theta}_4 \left[\mathbf{I}_3 \hat{\mathbf{z}}_3 + \overline{CC_3} \times (\hat{\mathbf{z}}_3 \times m_3 \overline{O_3 C_i}) \right. \\
& \left. + \sum_{i=8}^{9} \mathbf{I}_i \hat{\mathbf{z}}_3 + \sum_{i=8}^{9} \overline{CC_i} \times (\hat{\mathbf{z}}_3 \times m_i \overline{O_3 C_i}) \right]
\end{aligned} \tag{5}
$$

where $\mathbf{I}_i$ is the inertia tensor of link i, $\overline{O_j C_i}$ is a position vector from O_j to the center of mass C_i of link i, $\overline{CC_i}$ is the position vector from C to the center of mass C_i of link i and m_i is the mass of link i. We express this angular momentum in frame $\mathcal{F}_1$. Note that the inertia tensor ${}^{\mathcal{F}_i}\mathbf{I}_i$ is taken to be diagonal in the frame $\mathcal{F}_i$ with the expression

$$
{}^{\mathcal{F}_i}\mathbf{I}_i = \begin{bmatrix} I_{i1} & 0 & 0 \\ 0 & I_{i2} & 0 \\ 0 & 0 & I_{i3} \end{bmatrix}, \tag{6}
$$

where I_{i1}, I_{i2} and I_{i3} are the mass moment of inertias of link i along $\hat{\mathbf{x}}_i$, $\hat{\mathbf{y}}_i$ and $\hat{\mathbf{z}}_i$. This inertia tensor must be converted to $\mathcal{F}_1$. Appendix 1 provides some of the details used in the derivation. The scaled lengths $\$_i = O_i S_i$, $i = 1, 2, 3$ are shown in Fig. 3. In general, a position vector $\overline{CC_i}$ can be written as

$$
\overline{CC_i} = \alpha_i \hat{\mathbf{x}}_2 + \beta_i \hat{\mathbf{x}}_3 + \gamma_i \hat{\mathbf{x}}_4 \tag{7}
$$

https://doi.org/10.1017/S0263574704000670 Published online by Cambridge University Press

where α_i, β_i, and γ_i are functions of geometry and inertia parameters of the system. For details, please see reference [11].

Using the above relationship, it can be shown that the system angular momentum about the system center of mass $\mathbf{H}_C$ expressed in frame $\mathcal{F}_1$ is

$$\mathbf{H}_C = H^C_{x_1}\hat{\mathbf{x}}_1 + H^C_{y_1}\hat{\mathbf{y}}_1 + H^C_{z_1}\hat{\mathbf{z}}_1 \tag{8}$$

where $H^C_{x_1}$, $H^C_{y_1}$, $H^C_{z_1}$ are

$$\begin{aligned} H^C_{x_1} &= \dot{\theta}_1(A_1 s_2 c_2 + A_2 s_{23} c_{23} + A_3 s_{234} c_{234} - A_4 s_{223} \\ &\quad - A_5 s_{2234} - A_6 s_{23234}) \end{aligned} \tag{9}$$

$$\begin{aligned} H^C_{y_1} &= \dot{\theta}_1\big[(I_{11} + 2\overline{I}_{1a,1})s_2^2 + (I_{12} + 2\overline{I}_{1a,2})c_2^2 \\ &\quad + (I_{21} + I_{2a,1} + \overline{I}_{2a,1})s_{23}^2 + (I_{22} + I_{2a,2} + \overline{I}_{2a,2})c_{23}^2 \\ &\quad + (I_{31} + 2I_{3a,1})s_{234}^2 + (I_{32} + 2I_{3a,2})c_{234}^2 + m_1(-l_{*1}c_2 \\ &\quad + \$_2 c_2 + \$_2 c_{23} + \$_3 c_{234})^2 + m_2(-l_1 c_2 + \$_1 c_2 \\ &\quad - l_{*2}c_{23} + \$_2 c_{23} + \$_3 c_{234})^2 + m_3(l_1 c_2 - \$_1 c_2 \\ &\quad + l_2 c_{23} - \$_2 c_{23} + 2l_{*3}c_{234} - \$_3 c_{234})^2 + \overline{m}_{1a}\overline{l}^2_{1*a}c_2^2 \\ &\quad + \overline{m}_{1a}\$_3^2 c_{234}^2 - 2\overline{m}_{1a}\overline{l}_{1*a}\$_3 c_2 c_{234} + m_{2a}(l_{2*a}c_{23} \\ &\quad - \$_2 c_{23} - \$_3 c_{234})^2 + \overline{m}_{2a}(l_1 c_2 - s_1 c_2 + \overline{l}_{2*a}c_{23})^2 \\ &\quad + m_{3a}(l_1 c_2 - \$_1 c_2 + l_{3*a}c_{234} - \$_3 c_{234})^2 \\ &\quad + m_{3a}(l_{3*a} - \$_3)^2 c_{234}^2\big] \end{aligned} \tag{10}$$

$$\begin{aligned} H^C_{z_1} &= (A_7 + A_8 c_3 + 2A_5 c_{34} + 2A_6 c_4)\dot{\theta}_2 \\ &\quad + (A_9 + A_4 c_3 + A_5 c_{34} + 2A_6 c_4)\dot{\theta}_3 \\ &\quad + (A_{10} + A_6 c_4 + A_5 c_{34})\dot{\theta}_4 \end{aligned} \tag{11}$$

where a symbol such as $I_{2a,1}$ represents the moment of inertia of auxiliary link $2a$ along $\hat{\mathbf{x}}_3$, $\overline{I}_{1a,2}$ is the moment of inertia of auxiliary link $1\overline{a}$ along $\hat{\mathbf{y}}_2$, symbols shown in Fig. 3. Here, s_i, c_i, s_{ij}, c_{ij}, s_{ijk} and c_{ijk} stand for $\sin\theta_i$, $\cos\theta_i$, $\sin(\theta_i + \theta_j)$, $\cos(\theta_i + \theta_j)$, $\sin(\theta_i + \theta_j + \theta_k)$ and $\cos(\theta_i + \theta_j + \theta_k)$, respectively. Also, the links are considered to be slender such that the center of mass of a link i is located at a distance l_{*i} from its joint axis, $i = 1, 2, 3$. Moreover, the center of masses of auxiliary links $i\overline{a}$ is located at $\overline{l}_{i*a}$, $i = 1, 2$, and the center of mass of auxiliary link ia, $i = 2, 3$, is located at l_{i*a}.

All coefficients in the above equations are functions of geometric and inertial parameters of the links and are given in Appendix 2.

Using Eq. (4), one can derive the moment transmitted to the base given by

$$\mathbf{M}^C_1 = \frac{^{\mathcal{F}_0}d}{dt}\mathbf{H}_C = M^C_{x_1}\hat{\mathbf{x}}_1 + M^C_{y_1}\hat{\mathbf{y}}_1 + M^C_{z_1}\hat{\mathbf{z}}_1 \tag{12}$$

where

$$M^C_{x_1} = \left(\frac{d}{dt}H^C_{x_1} + H^C_{z_1}\dot{\theta}_1\right) \tag{13}$$

$$M^C_{y_1} = \frac{d}{dt}H^C_{y_1} \tag{14}$$

$$M^C_{z_1} = \left(\frac{d}{dt}H^C_{z_1} - H^C_{x_1}\dot{\theta}_1\right) \tag{15}$$

The moment $M^C_{z_1}$ is zero because of passive revolute joint at C. If $H^C_{x_1}$ and $H^C_{z_1}$ can be made to be zero, both $M^C_{x_1}$ and $M^C_{z_1}$ will vanish. However, it is impractical to make these terms identically zero. Hence, we adopt a two step procedure: (i) Select the geometric and inertial parameters such that $H^C_{x_1} = 0$, (ii) Choose the motion of the joints such that $H^C_{z_1} = 0$. Therefore, the only moment transmitted to the ground is M^C_{y1} exerted by the actuator at joint 1.

3.2. Design and planning of manipulator

It can be readily determined from Eq. (9) that the conditions required to vanish $H^C_{x_1}$ are

$$A_1 = A_2 = A_3 = A_4 = A_5 = A_6 = 0 \tag{16}$$

where A_i, $i = 1, \ldots, 6$ are given in Appendix 2. We choose the geometric and inertial parmeters of the links such that Eqs. (16) are satisfied. Since there are many unknowns and six equations to be set to zero, one uses approximate solution by using these geometric and inertial parameters. Upon solving these equations, it turns out that all equations are not exactly equal to zero. However, we may decrease these remaining terms by changing the geometric and inertia parameters.

Next, upon susbtitution of Eq. (16) in Eq. (11), one obtains

$$A_7\dot{\theta}_2 + A_9\dot{\theta}_3 + A_{10}\dot{\theta}_4 = 0 \tag{17}$$

Eq. (17) is a holonomic rate constraint equation on the motion of the last three joints of the parallelogram system. If joints 3 and 4 are actively driven, the motion of joint 2 is given as

$$\dot{\theta}_2 = -\frac{A_9}{A_7}\dot{\theta}_3 - \frac{A_{10}}{A_7}\dot{\theta}_4 \tag{18}$$

or

$$\theta_2 = -\frac{A_9}{A_7}\theta_3 - \frac{A_{10}}{A_7}\theta_4 + C_1, \tag{19}$$

where C_1 is a constant of integration. In summary, the moment transmitted to the base has only one component M^C_{y1}.

In the presence of a payload, we can consider two cases: (i) The mass of the payload is constant over the time, here, we can add this mass to the mass of last link and then design the reactionless system with new inertia parameters, (ii) The mass of payload is not constant, we can design the manipulator with auxiliary parallelograms such that the auxiliary links are telescopic and adjustable to account for the mass of the payload.

https://doi.org/10.1017/S0263574704000670 Published online by Cambridge University Press

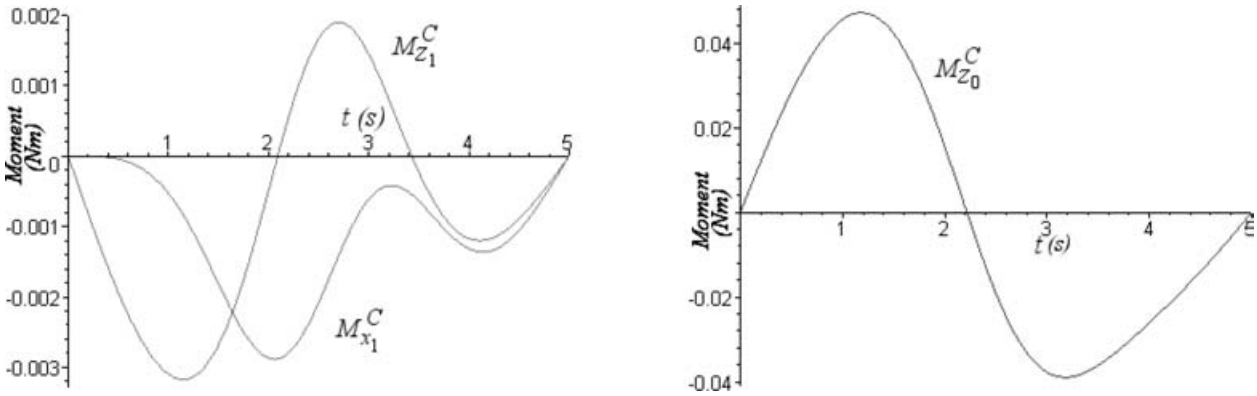

Fig. 4. Moments $M_{x_1}^C$, $M_{z_1}^C$ and $M_{z_0}^C$ for manipulator with auxilary parallelograms.

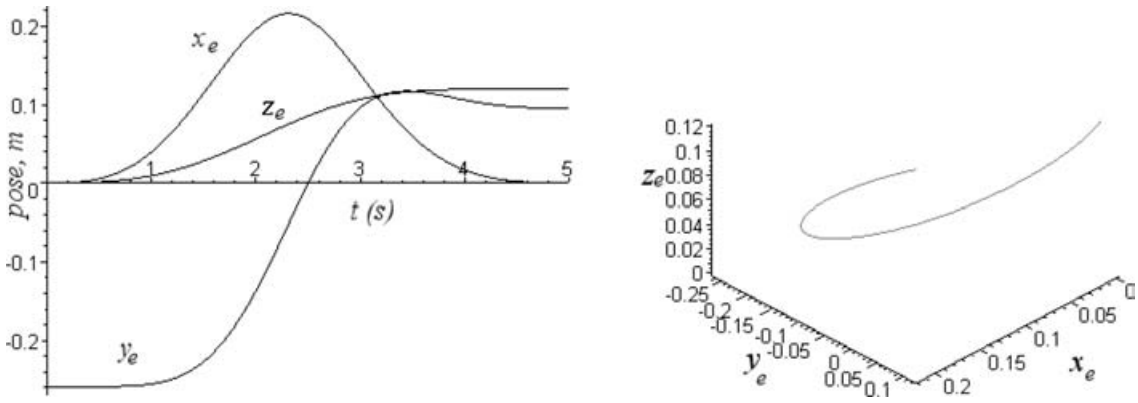

Fig. 5. End-effector trajectory in the inertial frame for manipulator with auxilary parallelograms.

4. NUMERICAL EXAMPLE

This section describes numerical example for model presented in Section 3. The task is to drive the manipulators from given positions and orientations of the end-effector to a desired final one. Note that only those end-effector orientations are allowed which can be obtained by rotation of the plane. Even though any motion can be chosen for the end-effector, we choose cycloidal motion for the joints. The moment transmitted to the base are computed using the procedure explained in Section 3.

The design of spatial 4-link manipulator satisfies the holonomic Eq. (18). Hence, only three out of four joints can be actively driven and the second joint is considered passive. The motion of first joint is independent of the other three joints. The actuated joints are assumed to have the following cycloidal motion

$$\begin{aligned} \theta_1 &= \theta_{10} + (\theta_{1f} - \theta_{10}) * s \\ \theta_3 &= \theta_{30} + (\theta_{3f} - \theta_{30}) * s \\ \theta_4 &= \theta_{40} + (\theta_{4f} - \theta_{40}) * s \end{aligned} \tag{20}$$

where θ_{i0} and θ_{if} are the initial and final values for θ_i and s is

$$s = \frac{1}{2\pi}\left[\frac{2\pi}{t_f}t - \sin\left(\frac{2\pi t}{t_f}\right)\right]. \tag{21}$$

t_f is the final time for the motion. Using Eq. (19), θ_2 is written in terms of θ_3 and θ_4. All angles are in radians. The boundary conditions are chosen such that the constants C_1 in Eq. (19) vanish. The motion of end-effector with respect to inertial frame can be written for the manipulator with auxilary parallelograms as

$$\begin{aligned} x_e =\ & \cos(\theta_1)[\bar{l}_{1a}\cos(\theta_2) + \bar{l}_{2a}\cos(\theta_2+\theta_3) \\ & + \bar{l}_{3a}\cos(\theta_2+\theta_3+\theta_4)] \\ y_e =\ & \sin(\theta_1)[\bar{l}_{1a}\cos(\theta_2) + \bar{l}_{2a}\cos(\theta_2+\theta_3) \\ & + \bar{l}_{3a}\cos(\theta_2+\theta_3+\theta_4)] \\ z_e =\ & \bar{l}_{1a}\sin(\theta_2) + \bar{l}_{2a}\sin(\theta_2+\theta_3) + \bar{l}_{3a}\sin(\theta_2+\theta_3+\theta_4) \end{aligned} \tag{22}$$

Using the above motion, one can also compute the time history of moments transmitted to the base using Eqs. (13), (14), (15), respectively.

As an example, the initial and final joint angles in Eqs. (20) are chosen as: $\theta_{10} = -\pi/2, \theta_{1f} = \pi/2, \theta_{30} = 0, \theta_{3f} = 2\pi/3, \theta_{40} = 0, \theta_{4f} = \pi/2$ and the time period is $t_f = 5s$.

4.1. Manipulator with auxilary parallelograms

The details of the geometric and inertial parameters for the manipulator with augmented parallelograms are: $l_1 = 0.2628$, $l_2 = 0.3329$, $l_3 = 0.1402$, $m_1 = 0.247023$, $m_2 = 0.53396$, $m_3 = 0.512472$, $m_{2a} = 0.113893$, $m_{3a} = 0.0892$,

https://doi.org/10.1017/S0263574704000670 Published online by Cambridge University Press

$\overline{m}_{1a} = 0.0369$, $\overline{m}_{2a} = 0.359926$, $\$_1 = .2445594804$, $\$_2 = .2087011776$ and $\$_3 = .02342699352$. All lengths and masses are expressed in MKS units. The time history of moments transmitted to the base are derived by inserting Eq. (22) into Eqs. (13), (14) and (15). The results are shown in Fig. 4. As shown, the moments tansmitted to base in $\hat{\mathbf{x}}_1$ and $\hat{\mathbf{z}}_1$ directions are very small but not equal to zero because of the approximate solution that we have used to satisfy Eq. (16) in Section 3.2. it may be noted that it is possible to obtain better result using different geometric and inertia parameters.

Figure 5 shows the time history of end-effector motion in the inertial frame using Eqs. (22).

5. CONCLUSION

The paper provided a systematic study of necessary and sufficient conditions for the design of classes of reactionless spatial robots. Detailed design and simulation were presented for spatial robots with open chains using auxiliary parallelograms. It was shown that these designs do not transmit any extra force to the base besides the gravity force. Also, through appropriate choice of geometric and inertial parameters and motion planning, the transmitted moment to the base has only one component in the direction of the actuated joint while the other two components of the moment identically vanish. In conventional designs of robots, manipulator motions result in forces and moments on the base, while the proposed methodology yields designs which will not cause undesirable reaction forces and moments to the base. We believe that these robots will be specially valuable in space robotics since manipulator motions will not create disturbances on the base thereby keeping the position and attitude of the base constant during motion.

Acknowledgments

The authors thank National Science Foundation for support of this work through "Presidential Faculty Fellows" program. The first author would also like to thank Isfahan University of Technology for its financial support during his sabbatical leave.

References

1. G. Lowen, F. R. Tepper and R. S. Berkof, "Balancing of Linkages – An Update", *Mechanisms and Machine Theory* **18**, No. 3, 213–220 (1983).
2. D. A. Streit and E. Shin, "Equilibrators for Planar Linkages", *Journal of Mechanical Design, Transactions of the ASME* **115**, No. 3, 604–610 (1993).
3. G. J. Walsh, D. A. Streit and B. J. Gilmore, "Spatial Spring Equilibrator Theory", *Mechanisms and Machine Theory* **26**, No. 2, 155–170 (1991).
4. H. Kazerooni, "Design and Analysis of the Statically Balanced Direct-Drive Robot Manipulator", *Robotics and Computer Integrated Manufacturing* **6**, No. 4, 287–293 (1989).
5. K. Youcef-Toumi and A. T. Y. Kuo, "Design and Control of a High-speed Direct-Drive Manipulator", *International Journal Prod. Research* **27**, No. 3, 287–293 (1989).
6. N. Ulrich and V. Kumar, "Passive Mechanical Gravity Compensation for Robot Manipulators", *Proc. of IEEE Int. Conf. on Robotics and Automation* (1991) pp. 1536–1541.
7. J. L. Herder and G. J. M. Tuijthof, "Two Spatial Gravity Equilibrators", *Proceedings, ASME Design Engineering Technical Conferences, MECH-14120* (2000) pp. 1–9.
8. T. Laliberte and C. Gosselin, "Static Balancing of 3 DOF Planar Parallel Mechanisms", *IEEE/ASME Transactions on Mechatronics* **4**, No. 4, 363–377 (1999).
9. J. Wang and C. M. Gosselin, "Static Balancing of Spatial three degrees-of-freedom Parallel Mechanisms", *Mechanisms and Machine Theory* **35**, 437–452 (1999).
10. A. Gokce and S. K. Agrawal, "Mass Center of Planar Mechanisms Using Auxiliary Parallelograms", *Journal of Mechanical Design, Transactions of ASME* **121**, No. 1, 166–168 (1999).
11. S. K. Agrawal, G. Gardner and S. Pledgie, "Design and Fabrication of a Gravity Balanced Planar Mechanism Using Auxiliary Parallelograms", *Journal of Mechanical Design, Transactions of the ASME* **123**, No. 4, 525–528 (2001).
12. C. Bagci, "Complete Shaking Force and Shaking Moment Balancing of Link Mechanisms Using Balancing Idler Loops", *Journal of Mechanical Design, Transactions of the ASME* **104**, 482–493 (1982).
13. R. S. Berkof and C. G. Lowen, "A New Method for Completely Force Balancing Simple Linkages", *Journal of Engineering for Industry* **91**, No. 1, 21–26 (1991).
14. R. S. Berkof and C. G. Lowen, "Theory of Shaking Moment Optimization of Force-Balanced Four-Bar Linkages", *Journal of Engineering for Industry* **93**, No. 1, 53–60 (1971).
15. V. H. Arakelian and M. R. Smith, "Complete Shaking Force and Shaking Moment Balancing of Linkages", *Mechanisms and Machine Theory* **34**, 1141–1153 (1999).
16. G. Feng, "Complete Shaking force and Shaking Moment Balancing of 26 types of Four-, Five- and Six-bar linkages", *Mechanisms and Machine Theory* **25**, 183–192 (1990).
17. R. Ricard and C. M. Gosselin, "On the Developement of Reactionless Parallel Manipulators", *Proceedings, ASME Design Engineering Technical Conferences, MECH-14098* (2000) pp. 1–10.
18. Y. Wu and C. M. Gosselin, "On the Synthesis of a Reactionless 6-DOF Parallel Mechanism using Planar Four-bar Linkages", *Proc. of Workshop on Fundamental Issues and future Research Directions for Parallel Mechanisms and Manipulators* (2002) pp. 310–316.
19. C. M. Gosselin and Y. Wu, "On the development of Reactionless Spatial 3-DOF Parallel-Piped Mechanisms", *Proc. of ASME Design Engineering Technical Conferences, MECH-34310* (2002) pp. 1–9.
20. S. Foucault and C. M. Gosselin, "On the development of a Planar 3-DOF Reactionless Parallel Mechanism", *Proc. of ASME Design Engineering Technical Conferences, MECH-34316* (2002) pp. 1–9.
21. E. Papadopoulos and A. Abu-Abed, "On the Design of Zero Reaction Manipulators", *Journal of Mechanical Design, Transactions of the ASME* **118**, No. 3, 372–376 (1996).
22. S. Dubowsky and M. A. Torres, "Path Planning for Space Manipulators to Minimize Spacecraft Attitude Disturbance", *Proc. of IEEE Int. Conf. on Robotics and Automation*, Sacramento, CA (1991) pp. 2522–2528.
23. D. N. Nenchev, K. Yoshida, P. Vichitkulsawat and M. Uchiyama, "Reaction Null-Space Control of Flexible Structure Mounted Manipulator Systems", *IEEE/ASME Transactions on Robotics and Automation* **15**, No. 6, 1011–1023 (1999).
24. K. Yoshida, K. Hashizume and S. Abiko, "Zero Reaction Maneuver: Flight Validation with ETS-VII Space Robot and Extension to Kinematically Redundant Arm", *Proc. of IEEE Int. Conf. on Robotics and Automation* (2001) pp. 441–446.
25. J. P. Karidis, G. McVicker, et al., "The Hummingbird Minipositioner– Providing Three-Axis Motion at 50 G's with Low Reactions", *Proc. of IEEE Int. Conf. on Robotics and Automation* (1992) pp. 685–692.

https://doi.org/10.1017/S0263574704000670 Published online by Cambridge University Press

APPENDIX 1

The inertia tensor $\mathbf{I}_i$ in frame $\mathcal{F}_1$ is derived as follows:

Upon substitution of Eq. (6) and in the light of expression for rotation matrix of frame $\mathcal{F}_i$ with respect to frame $\mathcal{F}_1$, namely,

$$^{\mathcal{F}_1}R_i = {}^{\mathcal{F}_1}[\,\hat{\mathbf{x}}_i\ \hat{\mathbf{y}}_i\ \hat{\mathbf{z}}_i] \tag{23}$$

one obtains

$$^{\mathcal{F}_1}\mathbf{I}_i = {}^{\mathcal{F}_1}[\hat{\mathbf{x}}_i(\hat{\mathbf{x}}_i)^T]I_{i1} + {}^{\mathcal{F}_1}[\hat{\mathbf{y}}_i(\hat{\mathbf{y}}_i)^T]I_{i2} + {}^{\mathcal{F}_1}[\hat{\mathbf{z}}_i(\hat{\mathbf{z}}_i)^T]I_{i3} \qquad i = 2, 3, 4 \tag{24}$$

where $\hat{\mathbf{x}}_i$, $\hat{\mathbf{y}}_i$ and $\hat{\mathbf{z}}_i$ in terms of unit vectors in frame $\mathcal{F}_1$ can be written as

$$\begin{aligned}
\hat{\mathbf{x}}_0 &= c_1\hat{\mathbf{x}}_1 + s_1\hat{\mathbf{z}}_1\\
\hat{\mathbf{y}}_0 &= s_1\hat{\mathbf{x}}_1 + c_1\hat{\mathbf{z}}_1\\
\hat{\mathbf{z}}_0 &= \hat{\mathbf{y}}_1\\
\hat{\mathbf{x}}_2 &= c_2\hat{\mathbf{x}}_1 + s_2\hat{\mathbf{y}}_1\\
\hat{\mathbf{y}}_2 &= -s_2\hat{\mathbf{x}}_1 + c_2\hat{\mathbf{y}}_1\\
\hat{\mathbf{x}}_3 &= c_{23}\hat{\mathbf{x}}_1 + s_{23}\hat{\mathbf{y}}_1\\
\hat{\mathbf{y}}_3 &= -s_{23}\hat{\mathbf{x}}_1 + c_{23}\hat{\mathbf{y}}_1\\
\hat{\mathbf{x}}_4 &= c_{234}\hat{\mathbf{x}}_1 + s_{234}\hat{\mathbf{y}}_1\\
\hat{\mathbf{y}}_4 &= -s_{234}\hat{\mathbf{x}}_1 + c_{234}\hat{\mathbf{y}}_1\\
\hat{\mathbf{z}}_i &= \hat{\mathbf{z}}_1 \quad i = 2, 3, 4
\end{aligned} \tag{25}$$

where s_i, c_i, s_{ij}, c_{ij}, s_{ijk} and c_{ijk} stand for $\sin(\theta_i)$, $\cos(\theta_i)$, $\sin(\theta_i + \theta_j)$, $\cos(\theta_i + \theta_j)$, $\sin(\theta_i + \theta_j + \theta_k)$ and $\cos(\theta_i + \theta_j + \theta_k)$, respectively.

APPENDIX 2

The coefficients of Eqs. (9) and (11) are as follows:

$$A_1 = I_{11} + 2\overline{I}_{2a,1} - I_{12} - 2\overline{I}_{2a,2} - A'_1 \tag{26}$$

$$A_2 = I_{21} + I_{2a,1} + 2\overline{I}_{2a,1} - I_{22} - I_{2a,2} - A'_2 \tag{27}$$

$$A_3 = I_{31} + 2I_{3a,1} - I_{32} - 2I_{3a,2} - A'_3 \tag{28}$$

$$A_4 = \overline{m}_{2a}(l_1 - \$_1)\overline{l}_{2*a} + m_3(l_1 - \$_1)(l_2 - \$_2) + m_2(l_1 - \$_1)(l_{2*} - \$_2) - m_1(l_{1*} - \$_1)\$_2 \tag{29}$$

$$A_5 = m_3(l_1 - \$_1)(l_{3*} - \$_3) - m_{3a}(l_1 - \$_1)(\$_3 - l_{3*a}) - m_2(l_1 - \$_1)\$_3 - m_1(l_{1*} - \$_1)\$_3 - \overline{m}_{1a}\overline{l}_{1*a}\$_3 \tag{30}$$

$$A_6 = m_3(l_2 - \$_2)(l_{3*} - \$_3) - m_2(l_{2*} - \$_2)\$_3 + m_1\$_2\$_3 + m_{2a}(\$_2 - l_{2*a})\$_3 \tag{31}$$

$$A_7 = A_1 + I_{c1,3} + 2\overline{I}_{1a,3} + A_9 \tag{32}$$

$$A_8 = 2A_4 \tag{33}$$

$$A_9 = A'_2 + A_{10} + \overline{I}_{2a,3} + I_{c2,3} + I_{2a,3} \tag{34}$$

$$A_{10} = A'_3 + I_{c3,3} + 2I_{3a,3} \tag{35}$$

where

$$A'_1 = m_1(\$_1 - l_{1*})^2 + m_2(l_1 - \$_1)^2 + m_3(l_1 - \$_1)^2 + m_{3a}(l_1 - \$_1)^2 + 2\overline{m}_{1a}l_{1*a}^{-2} + \overline{m}_{2a}(l_1 - \$_1)^2 \tag{36}$$

$$A'_2 = m_1\$_2^2 + m_2(\$_2 - l_{2*})^2 + m_3(l_2 - \$_2)^2 + m_{2a}(\$_2 - l_{2*a})^2 + \overline{m}_{2a}l_{2*a}^{-2} \tag{37}$$

$$A'_3 = m_1\$_3^2 + m_2\$_3^2 + m_3(\$_3 - l_{3*})^2 + m_{2a}\$_3^2 + 2m_{3a}(\$_3 - l_{3*a})^2 + \overline{m}_{1a}\$_3^2 \tag{38}$$

$$I_{ci,2} = I_{ci,3} = \frac{m_i l^2}{12} \quad i = 1, 2, 3 \tag{39}$$

$$I_{ia,2} = I_{ia,3} = \frac{m_{ia}\$_i^2}{12} \quad i = 1, 2, 3 \tag{40}$$

$$\overline{I}_{ia,2} = \overline{I}_{ia,3} = \frac{\overline{m}_{ia}(l_i - \$_i)^2}{12} \quad i = 1, 2, 3 \tag{41}$$

https://doi.org/10.1017/S0263574704000670 Published online by Cambridge University Press